LA-UR -82-2167

Conf-830104--3

LA-UR--82-2167

DE82 019532

TITLE: NUMERICAL SIMULATION OF FRACTURE

AUTHOR(S): L. G. Margolin, ESS-5

SUBMITTED TO: Proceedings of the International Conference on Constitutive Laws for Engineering Materials: Theory and Application January 10-14, 1983, at the University of Arizaon, Tucson, AZ

DISCLAIMER

MASTER

Los Alamos

Los Alamos National Laboratory
Los Alamos, New Mexico 87545

NUMERICAL SIMULATION OF FRACTURE

Leonard G. Margolin

Los Alamos National Laboratory
Los Alamos, NM 87545

SUMMARY. A constitutive model for brittle, and quasi-brittle materials is described. The Bedded Crack Model contains a microphysical description of fracture based on Griffith theory. The effect of cracks on material properties is described by effective modulus theory. Underlying the model is a statistical framework in which the evolution in time of a statistical distribution of cracks is calculated. The theory upon which the model is based is described.

The model is implemented in a finite difference computer code. Our model is contrasted with the phenomenologic models usually found in computer codes. A computational simulation of the strain rate dependence of failure stress is presented and compared with laboratory data. A simulation of a gas gun experiment is presented, and the mechanism of spall described.

INTRODUCTION

Computer simulation of stress wave propagation in geologic materials is a subject of growing importance. Interest is generated by such diverse programs as in situ recovery of fossil energy, prediction of earthquakes, cratering, and containment of underground nuclear explosions. The characterization of material behavior, and in particular of fracture, is a key element in building these computer models.

The Bedded Crack Model (BCM) is a constitutive model that has been developed for numerical simulation of fracture in a brittle, or quasi-brittle material. The BCM is based on a microphysical picture in which the evolution of a statistical distribution of penny shaped cracks is calculated. The BCM addresses two questions. For a material containing penny shaped cracks

1) how does the stress field affect the cracks - that is, when can cracks grow?
2) how do the cracks affect the material properties - that is, what are the effective moduli of a cracked material?

Intrinsic to the model is a statistical framework used to describe the distribution of cracks, as a function of size and orientation, as it evolves in time.

In the next section, we contrast the BCM with the phenomenologic models commonly used in computer simulations and point out some advantages inherent in a microphysical approach. We then briefly describe the theoretical basis of the model. Finally, we present numerical calculations using the BCM.

Previous papers (1,2,3) describe the use of BCM to simulate field events - for example, cratering experiments in oil shale where a typical length scale is tens of meters. In this paper, we will describe simulations of laboratory experiments. We will show that the BCM is inherently capable of predicting the dependence of fracture stress on strain rate without additional parameters. Also, we will show a simulation of a gas gun experiment and spall.

PHENOMENOLOGIC VERSUS MICROPHYSICAL MODELS

There are two aspects of modeling the fracture process. First, we must consider the effect of the stresses on the cracks. Second, we must allow for the effect of the cracks on the material properties, and on stress wave propagation through the material. These two aspects occur simultaneously and interactively, but on much different levels. The effect of stress on the individual cracks is a microscopic process. The effect of a statistical ensemble of cracks on material properties is a macroscopic process. The manner in which these two processes are related to each other allows a separation of computer models in two broad categories - phenomenologic and microphysical.

Phenomenologic models ignore the details of crack growth and concentrate on describing the effects of fracture on stress wave propagation. In the absence of knowledge about crack growth, a mathematical formalism analogous to plasticity theory is used. A material property called fracture stress is defined so that when the stress in the material exceeds the fracture stress, fracture "occurs" and the stress field is relaxed. The relaxation usually involves a second material parameter which is a characteristic time scale.

The concept of fracture stress as a material property is convenient and intuitively appealing. Unfortunately, it is not experimentally justified. Failure stress as measured in the laboratory is found to depend on many aspects of the experiment such as sample size and strain rate. Although the experimental results do not support the existence of a constant fracture stress, the results are quite consistent with Griffith theory which we will describe in the next section.

Microphysical models of fracture follow the growth of cracks and use this information to calculate effective elastic moduli for the medium. This class of models enjoys several advantages over phenomenologic models. To begin with, the input to a calculation consists of physically meaningful numbers, determined by experimental measurement. Because the model is based on physical processes and physical properties, it is capable of scaling from laboratory size experiments up to field experiments. An additional bonus is that detailed knowledge of crack statistics can become the basis of calculation of such properties as porosity, permeability and particle size distribution.

GRIFFITH THEORY

Much work has been done on the theory of fracture. Much of this effort builds on the original work of Griffith (4) and is based on two ideas:

1) Brittle materials contain microscopic flaws;
2) The stability of cracks under loading can be addressed in terms of a balance of energies.

The measured failure strength of brittle materials is often two orders of magnitude smaller than theoretical estimates based on breaking atomic bonds. Griffith postulated the existence of tiny flaws in the material. The mathematical solution for the stress field in the presence of a flaw shows that the flaw tips act as stress concentrators (5), drastically reducing the strength of the material. Furthermore, a statistical distribution of flaw density as a function of size and orientation is a material property which can be determined directly from section and counting.

Each microscopic flaw is really a tiny crack. It is crucial then to understand the conditions under which a crack can grow. Griffith's theory is based on the first and second laws of thermodynamics. For a virtual extension of the crack, Griffith compared the release of elastic strain energy (W) with the increase in surface energy (S). The surface energy is a macroscopic representation of the energy required to break atomic bonds. In these terms, the Griffith criterion states that a crack will grow if the energy release exceeds the energy required to grow the crack. Mathematically,

$$\frac{\partial}{\partial c}[W-S] \le 0$$

where c is the crack radius.

Griffith's analysis applies to two-dimensional slits in normal tension. We have generalized these results to three-dimensional cracks in a spatially uniform, but otherwise arbitrary external stress. For cracks in the x-y plane, where $_{zz}$ is positive (tensile), the crack will grow if

$$\sigma_{zz}^2 + \left(\frac{2}{2-\nu}\right)(\sigma_{xz}^2 + \sigma_{yz}^2) \ge \frac{4\pi TE}{c}$$

ν = Poisson's ratio
E = Young's modulus
T = coefficient of surface tension

Equation (2) shows that, in any external applied stress, there is a critical crack size. Cracks larger than critical are unstable to growth while smaller cracks are stable. The effect of shear stress is to decrease the critical crack size.

When σ_{zz} is negative (compressive), the crack is closed. In this case, the energy balance of equation 1 must include the additional energy dissipated by friction between the crack faces. Assuming the friction has the magnitude

$$\tau = \tau_0 - \mu\sigma_{zz}$$

where τ_0 is a cohesion and μ is the dynamic coefficient of friction. The crack can still grow in this case if

$$\frac{2}{2-\nu}[\sigma_{xz}^2 + \sigma_{yz}^2 - (\tau_0 - \mu\sigma_{zz})^2] \ge \frac{4\pi Te}{c}$$

The effect of friction is to increase the critical crack size. We note that friction may stabilize cracks even in the presence of large shear. We speculate that this is related to the brittle-ductile transition observed in many rocks (6).

EFFECTIVE MODULI

The presence of cracks alters the effective elastic moduli of the material. The effective moduli are found from static solutions for the displacement field for a body containing a statistical distribution of cracks and subjected to a spatially uniform, but otherwise arbitrary stress field (7). For example, for a material containing cracks bedded parallel to the x-y plane, the effective component of compliance C_{zzzz} is related to the compliance of the matrix material C^o_{zzzz} by

$$C_{zzzz} = C^o_{zzzz}/(1 + \frac{16}{3}(1-\nu^2)\gamma)$$

Here, γ is the third moment of the crack density distribution $N(c,t)$

$$\gamma = \overline{Nc^3} = \int_0^\infty N(c,t)\, c^3\, dc$$

The dimensionless number γ is really a measure of the amount of fracture. The inverse of the crack density is the volume per crack, and so is like the cube of the distance between cracks. Thus, γ is the cube of the ratio of crack size to crack spacing. When γ is approximately equal to 1, the cracks are about as big as they are far apart. We interpret this as fragmentation. The results of Hoenig (7) show that the effective moduli of a randomly cracked material are reduced to zero at $\gamma = 9/16$.

In the modulus calculation, γ plays the role of an expansion parameter. To lowest order, the interactions between cracks are ignored. For larger values of γ, crack interactions are accounted for by a self-consistent calculation. The self-consistent method (7) presupposes knowledge of the crack distribution. In particular, a spatially random distribution is usually assumed. This cannot be a reasonable assumption as approaches 9/16. Indeed, one can see that this effect of crack intersections must be second order (γ^2).

The details of self-consistent corrections to the effective module are probably not important for calculations of stress wave propagation. However, they may play an important role if one is interested in using the crack statistics to calculate fragment size.

The effective modulus theory predicts a reduced elastic compliance for a cracked body. A more accurate picture for stress wave propagation is contained in elastic scattering theory. Consideration of the scattering of a wave from a penny shaped crack leads to a dispersion relation (8) and shows that the dynamic effective moduli are complex. The imaginary part represents the attenuation of the wave due to energy loss in the scattering process.

Computer modeling of the attenuation is difficult, for the attenuation is frequency dependent. However, the analysis (8) shows that the attenuation of these amplitude is smaller than the change in modulus by an additional factor of $(kc)^3$ where k is the wave number. This represents a small effect in most calcualtions and is ignored.

As the cracks grow the distribution evolves and so γ and the effective moduli vary in time. The constitutive relation takes the form

$$\frac{d\epsilon_{ij}}{dt} = \frac{d}{dt}[C_{ijkl}\sigma_{kl}]$$

or

$$\frac{d\sigma_{kl}}{dt} = (C^{-1})_{klij}\, [\frac{d\epsilon_{ij}}{dt} - \dot{C}_{ijmn}\sigma_{mn}]$$

Thus, the constitutive relation has the form of a Maxwell solid, but with a variable relaxation time.

SIZE AND STRAIN RATE EFFECT

Laboratory measurements of failure stress show a dependence on sample size. This result is easily understood in terms of Griffith theory. Equation 2 may be interpreted as saying that big cracks will commence to grow at lower stress levels than smaller cracks. Statistically, bigger samples are more likely to contain bigger cracks. For example, a five centimeter sample cannot contain a six centimeter crack, whereas a ten meter sample could easily contain a six centimeter crack.

A further analytic result (9) is that cracks have an asymptotic speed of growth which is a fraction (1/3 to 1/2) of the shear wave speed. The existence of this limit leads to a strain rate dependence of failure stress. No matter how fast the material is loaded, crack growth and consequent stress relaxation (equation 8) is limited. Thus, at higher strain rate, a larger stress will be tolerated before the cracks grow sufficiently to relax the stress.

Figure 1 - A plot of fracture stress vs. strain rate for oil shale. The triangles are the experimental data of Grady and Kipp (10). The solid line represents computer simulations with the BCM. The two points at about 10 sec^{-1} represent tests along, and across the bedding planes. Results at higher strain rates are not sensitive to orientation with respect to the bedding planes.

This effect is shown in figure 1. The data are from Grady and Kipp (10). The solid line represents the BCM simulation of a tensile failure test. In the simulation, we assumed an exponential size distribution - the number of cracks with radius greater than c is

$$N_0 \exp(-c/\bar{c})$$

The results of figure 1 use only the fracture parameters N_0 and c, the fracture toughness (which is equivalent to the constant T in equation 2) and the elastic constants.

Figure 2 - Stress-strain curves for oil shale for three strain rates. These curves were generated by the BCM, and their maxima are points on the solid curve of figure 1. Note that the relaxation after failure is steeper for smaller strain rates.

SPALLATION

The BCM has been inserted into a two-dimensional stress wave code SHALE. The code was used to study spallation in gas gun experiments in terms of crack growth. We simulated a gas gun experiment in which a cylindrical sample of oil shale was impacted by a high-speed projectile. The sample (figure 3) was 4 cm long and 1 cm in diameter. We assumed the cracks were bedded in planes that were perpendicular to the cylindrical axis. As a result of the impact, a compressive pulse was generated, travelled down the axis toward the free surface at the other end of the sample, and was reflectd as a tensile wave. The wave was about 1 cm in width and -10 kbar in amplitude (figure 4). Details of the reflection of this pulse from the free surface are shown in figure 5.

Figure 3 - A cylindrical sample of oil shale for a gas gun simulation. The bedding planes are perpendicular to the cylindrical axis - this is, vertical in this figure.

Figure 4 - The stress pulse generated by impact is shown. The horizontal axis is distance along the sample axis. The pulse is approximately a square wave, and is negative which is compressive by our convention.

The growth of cracks in the sample as a result of the reflected pulse can be described in terms of which is defined in equation 6. Figure 5 shows as a function of position in the sample as computed by BCM. The sharp peak represents the large growth of cracks in this region, leading to a separation plane and a spall layer. The spall layer is approximately half as wide as the incoming pulse.

Figure 5 - The stress pulse is shown in three stages of its reflection from the free surface at the end of the sample. Geometric construction is consistent with the emergence of the first significant tension about one half wave length from the free surface.

The spallation process, as simulated by BCM, can be described as follows. In general, cracks can grow in tension, shear, or a combination of the two as described by our generalized Griffith criteria (equations 2 and 4). Because of the simple geometry and the assumed orientation of the cracks in the sample, tension is the only means of causing crack growth. Figure 5 shows that during the reflection of the wave from the free surface, no significant tensions develop closer to the free surface than about one-half pulse width away. Therefore, there is little or no crack growth in the spall layer. Where tensions do develop, the crack growth is rapid and the fracture process attenuates the reflected tensile wave, producing the sharp peaks in shown in figure 6. The sharp peak indicates a small region of intensely cracked material which has no strength - the effective modulus relating stress to strain (equation 5) is very small. This region represents the separation plane.

Figure 6 - The dimensional number γ is plotted along the sample axis. The steep peak is associated with large crack growth due to the first emergence of the tensile relief wave. Separation can be expected at this spot, leading to spallation.

THE SHALE CODE

The BCM has been implemented in the two-dimensional stress wave code SHALE. SHALE is a finite difference code based on the "ALE" method (11) in which the computational mesh may have an arbitrary velocity with respect to the material. Particular cases are the familiar Lagrangian calculations in which the mesh moves with the material, and Eulerian calculations which employ a fixed mesh.

In general, Lagrangian calculations are preferred because they introduce the least numerical diffusion into the results. However, in problems with large deformations, Lagrangian cells distort, causing loss of accuracy in the difference approximations. In this situation, the computational time step (which is based on a Courant Stability Criterion) becomes very small, making calculations very expensive or even impractical.

The "ALE" method provides a powerful alternative to Lagrangian mesh tangling and to Eulerian diffusiveness. The calculation is run in a Lagrange fashion until the mesh begins to distort. Then a continuous rezoner is employed which prevents tangling and consequent loss of accuracy. The computer program is smart enough to allow rezoning only where it is necessary.

Two problems arise in the simulation of wave propagation in solids which are not important for wave propagation in fluids. Both problems are associated with the use of a constitutive relation in place of an equation of state. The distinction that we make is that a constitutive relation relates stress rate to strain rate, thus allowing a dependence of the state on the history of the loading.

The first problem is associated with the use of artifical viscosity (12) to represent shock waves. The artifical viscosity smears the numerical precursor to the shock over three or four computational cells. (The viscosity is artifical because it scales with mesh spacing which is not a physical quantity.) Because all cracks grow with the same asymptotic speed, the shape of the precursor plays an important role in determining the amount of fracture ahead of a shock.

The artifical viscosity can also change the prediction of the spall plane location. Our calculations in the previous section show that the spall depth is half the wavelength of the incoming pulse. If artificial viscosity is allowed to smear the pulse too greatly, it will also affect the spall depth. The cure for these effects of artifical viscosity is to use sufficiently fine computational meshes. The "ALE" technique can be beneficial here if the rezoner is used to let fine zones follow the shock.

The second problem found in solid dynamic calculations is related to numerical stability. Mathematically, SHALE numerically integrates a coupled set of partial differential equations. The stability of the integration leads to restrictions on the size of the computational time step such as the well-known Courant condition.

The use of a constitutive relation adds another partial differential equation to the set and alters the stability. Hicks has shown (13) that the stability of the calculation requires the time step to be a fraction of the relaxation time in equation (8). This condition is simple to implement, but is not well known.

REFERENCES

(1) Margolin, L.G., "Calculations of Cratering Experiments with the Bedded Crack Model," Proc. of the APS Symposium on Shock Waves in Condensed Matter, Menlo Park, California, July 1981.

(2) Dienes, J. K. and Margolin, L. G., "A Computational Approach to Rock Fragmentation," Proc. of the 21st U.S. National Symposium on Rock Mechanics, Rolla, Missouri, May, 1980.

(3) Margolin, L. G. and Adams, T. F., "Numerical Simulation of Fracture," Proc. of the 23rd U.S. National Symposium on Rock Mechanics, Berkeley, California, August, 1982.

(4) Griffith, A. A., "The Phenomena of Rupture and Flow in Solids," Philosophcal Transactions of the Royal Society A, Vol. 221, 1920, pp. 137-154.

(5) Orowan, E., "Energy Criteria of Fracture," Welding J. Supp. Vol 34, 1955, pp 157-160.

(6) Byerlee, J. D., "Brittle-Ductile Transition in Rocks," J. Geophys Res. V 73, 1968, pp 4741-4750.

(7) Hoenig, A., "Elastic Moduli of a Nonrandomly Cracked Body," International Journal of Solids and Structures," Vd. 15, 1979, pp 137-154.

(8) Dunlanev, E. N. and Brace, W. F., "Velocity Behavi of a Growing Crack," Journal of Applied Physics, Vol. 31, pp. 2133-2236, 1960.

(9) Piau, M., "Attenuation of a Plane Compressional Wave by a Random Distribution of Penny Shaped Cracks," Int. J. Engineering Science, Vol. 17, pp. 152-167, 1979.

(10) Grady, D. E. and Kipp, M. E., "Continuum Modelling of Explosive Fracture in Oil Shale," Int. J. Rock Mech. Min. Sci. and Geomech. Abst. Vol. 17, pp. 147-157, 1980.

(11) Amsden, A. A., Ruppel, H. M. and Hirt, C. W., "SALE: A Simplified ALE Computer Program for Fluid Flow at All Speeds," Los Alamos National Laboratory Report LA-8095, June, 1980.

(12) Wilkins, M. L., "Use of Artificial Viscosity in Multi-Dimensional Fluid Dynamic Calculations," J. Comp. Physics, Vol. 36, pp. 281-303, 1980.

(13) Hicks, D. L., "Stability Analysis of the Von Neumann-Richtmyer Difference Scheme with Rate Dependent Material Relations," Sandia National Laboratory Report SAND-76-0634, February, 1977.

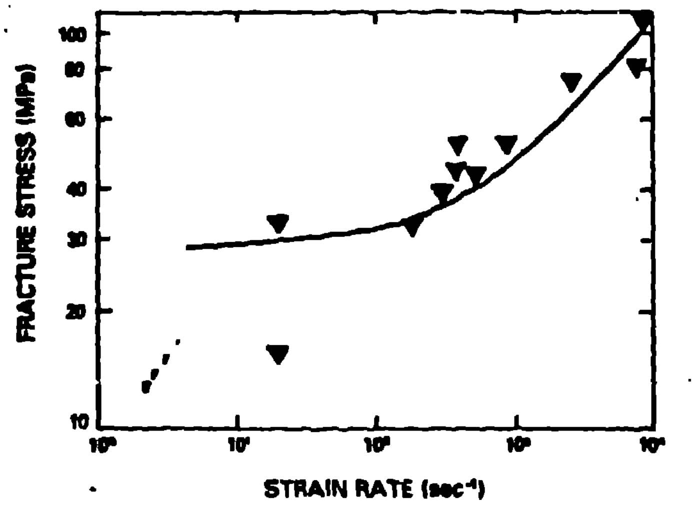

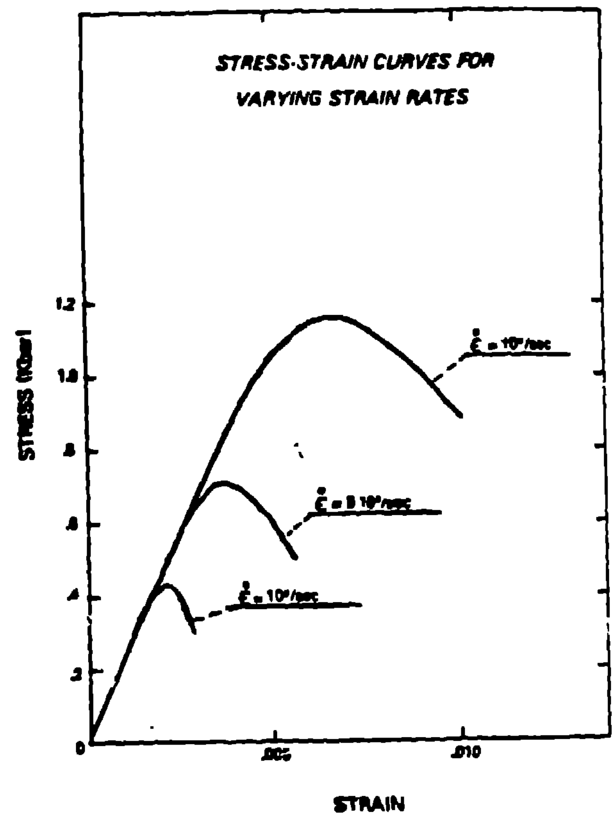

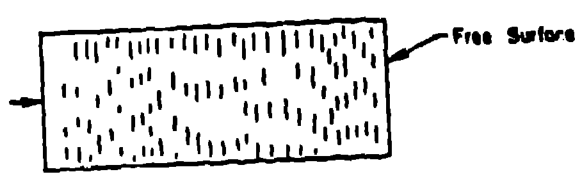

Cracks are bedded perpendicular to cylinders axis

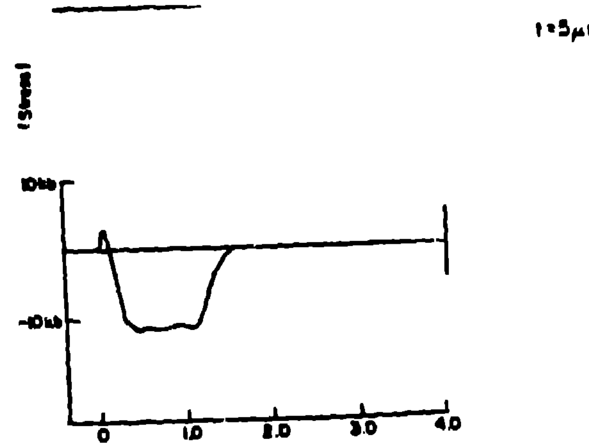

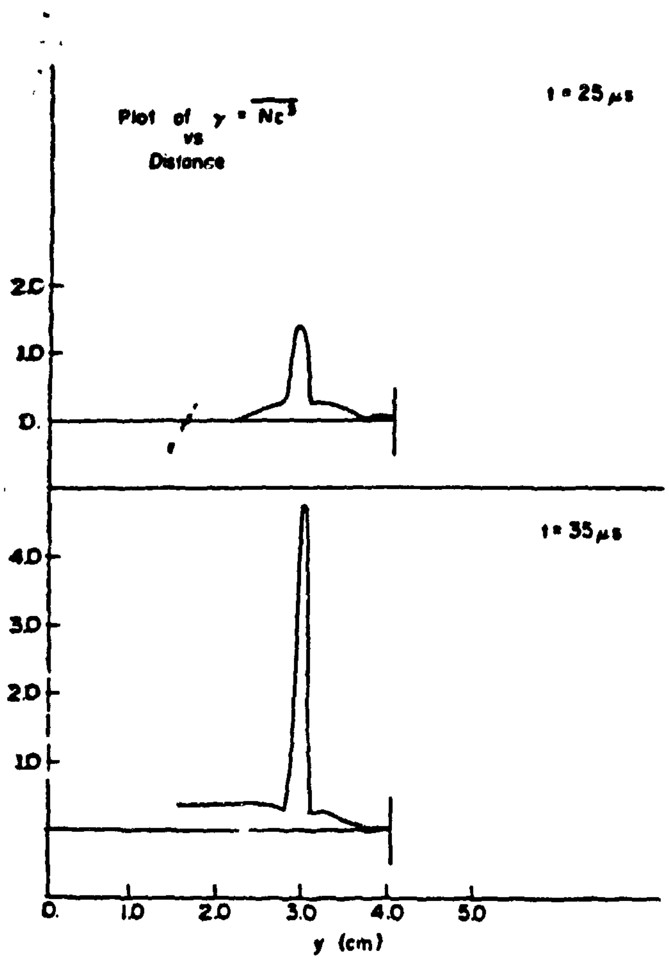
t = 25 μs
Plot of γ = $\overline{Nc^3}$
vs
Distance
2.0
1.0
0.
t = 35 μs
4.0
3.0
2.0
1.0
0.
1.0
2.0
3.0
4.0
5.0
y (cm)

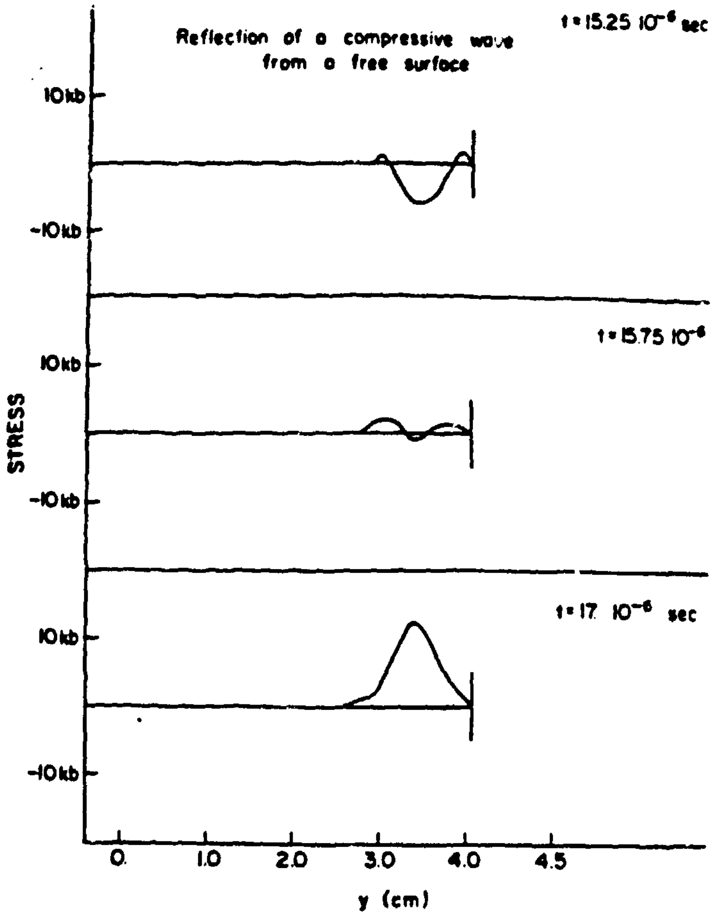
t = 15.25 10^{-6} sec
Reflection of a compressive wave
from a free surface
10kb
-10kb
t = 15.75 10^{-6}
10kb
STRESS
-10kb
t = 17 10^{-6} sec
10kb
-10kb
0.
1.0
2.0
3.0
4.0
4.5
y (cm)